Heliyon 10 (2024) e32161

Contents lists available at ScienceDirect

Heliyon

journal homepage: www.cell.com/heliyon

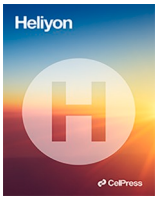

Research article

Effects of high gravity on properties of parts fabricated using material extrusion system by additive manufacturing

Xin Jiang [a,b], Ryo Koike [b,*]

[a] Research and Development Department, Kanagawa Institute of Industrial Science and Technology, 705-1 Shimoimaizumi, Ebina, Kanagawa, 243-0435, Japan
[b] Department of System Design Engineering, Keio University, 3-14-1 Hiyoshi, Kohoku-ku, Yokohama, Kanagawa, 223-8522, Japan

ARTICLE INFO

Keywords:
Additive manufacturing
High gravity
Fabricated parts
Material extrusion

ABSTRACT

Additive manufacturing (AM) has gained significant attention in recent years owing to its ability to fabricate intricate shapes and structures that are often challenging or unattainable using conventional manufacturing techniques. This high-quality development trend entails higher requirements for the structural design of 3D printers. In this study, polylactic acid (PLA) and acrylonitrile butadiene styrene (ABS) filaments were fed through a heated extrusion nozzle, which melted the material and deposited it onto a build platform. This study's objectives are high-gravitational material extrusion (HG-MEX) systems development, analyzing the high gravity influences on the flow behavior of materials during extrusion, and understanding the effects of gravitational on material flow and overall extrusion performance. HG-MEX systems have great potential for addressing various challenges in additive manufacturing, such as precise manufacturing. The highlight of the progress is that we developed an HG-MEX system and applied surface science to material extrusion in different gravity. We established a system and obtained results on different gravity, we analyzed the analogy between different gravity phenomena. We analyzed the interplay between the behavior of the fabricated parts and gravity. We analyzed high gravity effects on extrusion processes. The results confirmed the characteristics and feasibility of the developed system. The results suggest that a material extrusion line operating under 15 G conditions resulted in better printing quality compared to one operating under 1 G conditions. This observation implies that high gravity had a positive effect on the extrusion process, leading to improved material extrusion performance.

1. Introduction

Additive manufacturing (AM) involves the construction of three-dimensional objects by incrementally adding layers of material. The growing social and economic importance of AM has led to increased research and development in this field [1]. The development of AM printing technology is rapidly advancing worldwide, with researchers continuously exploring new technologies and products [2–5]. The development of AM equipment has been a key driving force in 3D printing. Over the years, there has been significant progress in improving the performance, precision, speed, and reliability of AM equipment [6–8]. These advances have accelerated the adoption of 3D printing, expanding its capabilities and unlocking new possibilities for design, manufacturing, and customization. The

* Corresponding author.
E-mail address: koike@sd.keio.ac.jp (R. Koike).

https://doi.org/10.1016/j.heliyon.2024.e32161
Received 14 December 2023; Received in revised form 27 May 2024; Accepted 29 May 2024
Available online 31 May 2024

research in AM equipment, enhancing the overall performance, efficiency, and versatility of 3D printing technology. Fused deposition modeling (FDM) is a popular AM printing technology which can build objects layer by layer [9–11].

The development and evolution of MEX equipment are crucial in improving the capacities and dependability of AM techniques [12–15]. The material extrusion system in MEX printers is a critical component [16–18], which has undergone significant advancements. These extruder systems are responsible for melting, controlling flow, and accurately extruding thermoplastic filaments during printing. Exploring the impact of high gravitational forces on the properties of parts fabricated using material extrusion systems is gaining increasing attention [19,20]. The ability to manipulate the influence of gravity during the additive manufacturing process can revolutionize the production of intricate components. The material extrusion in various gravity levels has different structural, mechanical, and thermal properties.

In material extrusion, the Eötvös number is a dimensionless quantity that relates the effects of surface tension to the gravitational forces acting on a liquid [21,22]. Furthermore, it is used to understand how the surface tension influences the material extrusion in different gravity [23–25]. Surface tension is a cohesive force that exists at the interface of different phases. The surface tension of a material affects various aspects of the printing process [26]. Cowley A. et al. [27] studied effects of variable gravity conditions on additive manufacture by fused filament fabrication using polylactic acid thermoplastic filament. The findings suggest that variations in gravity alter the stability of the extruded filament, affecting its shape, orientation, and bonding with previously deposited layers. Higher gravity levels may promote better filament deposition and layer adhesion due to increased pressure and reduced filament sagging or deformation. Jahromi P F et al. [28] studied pressure-driven liquid-liquid separation in Y-shaped microfluidic junctions. Higher gravity could enhance material flow rates, promote more uniform filament extrusion, and improve surface wetting and adhesion on substrate surfaces. Amin et al. [29] fabricated superhydrophobic PLA surfaces by tailoring FDM 3D printing and chemical etching processes. Chen et al. [30] studied the modification of surface quality and mechanical properties by laser-polishing Al/PLA parts manufactured by fused deposition modeling. Moreover, Miguel et al. [31] analyzed the contact angle of impacting droplets using a polynomial fitting approach.

The gravitational effect can significantly affect the AM-printed shape and dimensional accuracy of printed objects [32–34]. High-gravity AM is a relatively new technology that uses centrifugal force to print objects [35–37]. The high-gravity field of AM research poses challenges in producing high-performance parts. However, these high-gravity areas offer opportunities for research and development to explore new printing techniques and material behaviors and to optimize the AM process under different gravitational environments. High-gravity conditions can affect the flow and deposition of materials, material compaction, and layer adhesion during AM processes, potentially enhancing the material properties, density, strength, and print quality. By understanding the effect of gravity on AM, scientists and engineers can expand the capabilities of 3D printing technology in various fields. As high-gravity AM technology advances, the unique properties imparted by high-gravity conditions can be leveraged. HG-MEX indeed opens doors to advanced applications that extend beyond traditional manufacturing [38–41]. This technology has the potential to revolutionize space exploration through the on-site manufacturing of critical components and structures essential for spacecraft, habitats, and satellites. Moreover, in the realm of biomedical engineering, HG-MEX holds promise in enhancing patient care and advancing medical device production. Furthermore, HG-MEX facilitates research endeavors in materials science, fluid dynamics, and process optimization, thereby empowering scientists and engineers to devise novel solutions to real-world challenges. With its adaptable nature, HG-MEX serves as a versatile platform for exploring advanced applications across various sectors, encompassing space exploration, healthcare, and renewable energy. Consequently, by pushing the boundaries of additive manufacturing technology, HG-MEX lays the foundation for fostering innovation, promoting sustainability, and driving economic growth in the 21st century. Fig. 1 shows the differences between the MEX method for different gravity values.

This study delves into the development and characterization of HG-MEX system, aimed at pushing the boundaries of AM technology. This system with a peak output of 15 G, where 1 G corresponds to 9.81 m/s^2. Specialized equipment and facilities were developed to create specific gravity conditions for Additive Manufacturing (AM) in high-gravity fields. We found the impact of

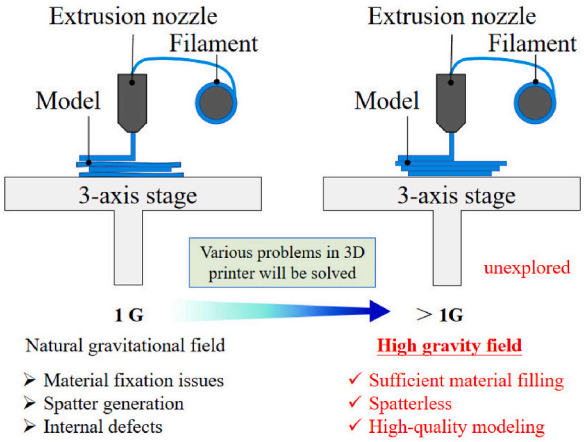

Fig. 1. Differences in the MEX method with different gravity.

increased gravitational acceleration on the fabrication process of single-line components, providing significant insights into the performance and feasibility of the proposed HG-MEX system under high-gravity conditions. Additionally, it presents the design and primary experimental results of an HG-MEX system under high gravity (15 G). The characteristics of extruded PLA and ABS materials under varying gravity conditions are summarized, yielding valuable insights into the performance and feasibility of the proposed HG-MEX system under high-gravity conditions. The results confirm the characteristics and feasibility of the proposed HG-MEX system. By analyzing these characteristics and experimentation at various gravity levels, we demonstrated the effectiveness of high gravity. We found the efficacy of high gravity in augmenting material extrusion processes. The investigation into HG-MEX signifies a potential breakthrough in plastic additive manufacturing technologies. The capacity to produce components with heightened precision, structural integrity, and dimensional accuracy within high-gravity environments holds substantial promise for transforming numerous industries.

2. Materials and methods

2.1. High gravity in fused deposition modeling

To design an effective HG-FDM system, comprehensive attention is required to each constituent element. An apparent centrifugal force emerges when the object moves along a circular trajectory [39]. Fig. 2 presents the surface tension with gravity in material extrusion.

To facilitate the discharge of the molten resin through the outlet hole, we counteracted and surpassed the cohesive force of the surface tension. In Fig. 2, P is the extrusion pressure, and G is the gravity in the small-diameter holes. The Eötvös number E_0 is expressed using the following equation (1):

$$E_0 = \frac{g\Delta\rho a^2}{\gamma} \tag{1}$$

where $\Delta\rho$ is the density difference, g is the gravitational acceleration, a is the hole diameter, and γ is the surface tension of the droplet geometry. We delved into the scaling effects under conditions of n- or n^2-times gravity, which led to the formulation of a set of similarity principles termed "Analogous Gravitational Field Relationships," introduced by Koike [36,37]. These principles were applied in a consistent manner. By incorporating the gravitational influences into the design and procedural considerations, we examined the gravitational implications and achieved heightened precision and dependability in outcomes.

The drop profile within a suspended liquid was influenced by both gravitational and surface forces. Additionally, we considered the impact of these forces on the geometry and analyzed. This tensile force arose from the surface tension along the circumference of the liquid droplet.

Fig. 3 presents schematic of liquid drop showing the quantities in Young's equation. The Young equation describes the relationship between the contact angle (θ_C), the surface tensions of the involved phases (σ), and the interfacial tension (γ) at the three-phase contact point of a liquid drop on a solid surface. Thus, we obtain Equation (2).

$$\gamma_{SG} = \gamma_{SL} + \gamma_{LG} \cdot \cos(\theta_C) \tag{2}$$

where γ_{SG} is the solid-vapor interfacial tension, γ_{SL} is the solid-liquid interfacial tension, and γ_{LG} is the liquid-vapor interfacial tension. We obtain the following modified Young's equation (3):

$$\cos(\theta_C) = \frac{\gamma_{SG} - \gamma_{SL}}{\gamma_{LG}} + \frac{k}{\gamma_{LG}}\frac{1}{a} \tag{3}$$

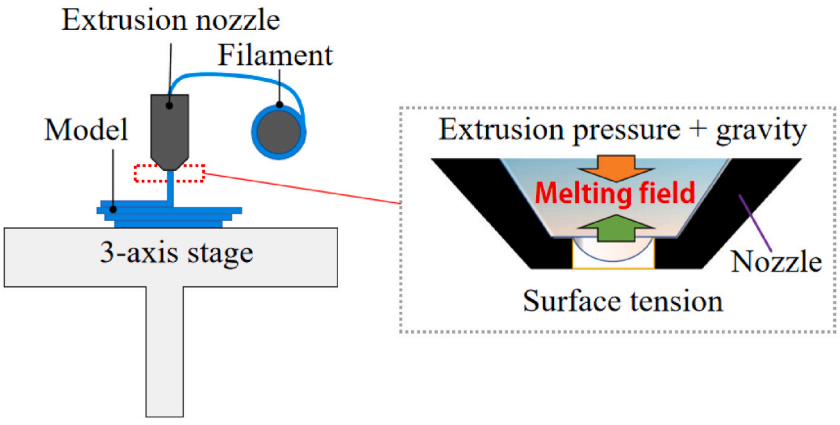

Fig. 2. Surface tension and gravity in material extrusion.

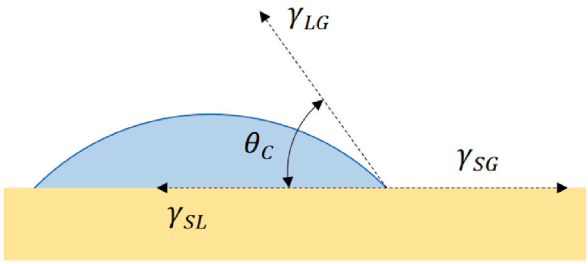

Fig. 3. Schematic of liquid drop showing the quantities in Young's equation.

where k is the line tension, and a is the droplet radius.

In a liquid drop scenario, Young's equation related the interfacial and contact angle values to explain the equilibrium configuration of the drop on a solid surface. If the contact angle is small, the liquid wets the surface more readily, and the liquid drops spread. If the contact angle was large, the liquid beaded up and did not spread as much.

In the equilibrium configuration, the droplets formed a distinct shape with a curved interface. The balance between the downward pull of gravity and the upward resistance of the surface tension defined the drop profile. By analyzing the shape and dimensions of the pendant drop, we derived information regarding the surface tension and other properties of the liquids under investigation. Furthermore, this method is widely used in fields such as materials science, fluid dynamics, and chemistry to understand liquid behavior and intermolecular forces.

2.2. Materials of filament

PLA and acrylonitrile butadiene styrene (ABS) are widely used thermoplastic materials in the MEX field [42,43]. They are commonly used to create diverse shapes and geometries. The properties of printed parts can be influenced by material extrusion conditions and modifying these conditions can assist in attaining the desired properties for specific applications [44,45]. In MEX, different gravity has different quality. This effect became more noticeable when printing overhanging structures.

2.3. HG-MEX methodology

We developed an HG-MEX system. The MEX unit is of the vertical axial type for rotating exercises. The centrifugal acceleration a_c [m/s^2] is shown in equation (2):

$$a_c = r_s w_s^{\,2} \tag{2}$$

Where r_s [m] is the distance from the center of the rotating body to build surface and w_s [rad/s] is the rotational speed. The rotation speed of N [min^{-1}] is shown in equation (3):

$$N = \frac{60 w_s}{2\pi} = \frac{30 w_s}{\pi} \left(w_s = \frac{N\pi}{30} \right) \tag{3}$$

The resultant acceleration a_r [m/s^2] is expressed as shown in equation (4):

$$a_r = \sqrt{a_c^{\,2} + a_g^{\,2}} \tag{4}$$

where the centrifugal acceleration is a_c [m/s^2] and a_g [m/s^2] is the natural gravitational acceleration (1G) in the direction perpendicular to the earth surface. In addition, the relationship between the resultant acceleration and rotation speed N [min^{-1}] is expressed as shown in equation (5):

$$N = \frac{2\pi}{60} \sqrt{\frac{\sqrt{a_r^{\,2} - a_g^{\,2}}}{r_s}} \tag{5}$$

We conducted research of high gravity fields.

3. Experiment setup

3.1. Fabrication apparatus

A new experimental environment was prepared for installation, including a mechanism designed to be mounted on high-gravity centrifuge machines. The proposed HG-MEX equipment was developed by analyzing a high gravitational field.

We designed a robot controller for the nozzle movement of the nozzle and developed control parts for HG-FDM. Communication

software was used to control and interact with robots when programming, monitoring, and configuring their behavior. This software provides a user interface that allows operators, engineers, or programmers to interact with the robots by sending commands, receiving feedback, setting parameters, or monitoring the status of the robot. Fig. 4 presents schematics of the developed HG-MEX machine.

Single-axis robots in the HG-MEX move along one linear axis. Supplying the controller with single-axis robots provides a convenient solution for using robots under high gravity. Designing robots to work in a high-gravity system was challenging because increased gravitational forces can affect the stability and power requirements of the robot. High gravity requires the robot to operate for extended performance-intensive tasks, necessitating the design of a power supply system capable of meeting increased power demands. We obtained the movable space for the robot and nozzle movement by measuring the HG-FDM system. Fig. 5 shows schematics of the HG-MEX machine used in this study.

3.2. Fabrication conditions and properties

In HG-MEX, the combined centrifuge machine and MEX unit require specialized design and engineering to ensure compatibility and synchronization. The rotating machine consists of a motor or engine driving a rotating element, such as a rotor or drum, spinning around the central axis. Combining the centrifuge machine and an MEX unit is preferable for economic reasons. In this study, we designed the specific characteristics of a rotating machine using a 0.4 mm nozzle. By manipulating the motor speed, the rotation state of the machine can be customized to suit the desired application, process, or experimental conditions, generating different gravitational fields.

4. Results and discussion

4.1. Evaluation for fabricated parts

By viewing the PLA coming out of the nozzle with the single-axis robot movement, the material extrusion process is almost similar. We considered a nozzle for the bottom plate at a distance of 0.4 mm. The high-gravity field line size is different owing to the impact of the amount of material extrusion and the movement speed of the nozzle. Fig. 5 shows material extrusion with single-axis robot movement.

Material extrusion characteristics were obtained using a single-axis robot in the HG-MEX system. Fig. 5 illustrates material extrusion in the HG-MEX system. This system comprises several essential components, including a heater, nozzle, and build platform. The heater's function is to elevate the thermoplastic material to its melting point or within its processing temperature range, ensuring its molten state for extrusion through the nozzle onto the build platform. The nozzle, responsible for extruding the molten thermoplastic material onto the build platform, determines the filament's diameter and shape. The extruder was mounted on a single-axis robot, and the filament was heated and melted. As the robot moved along the linear axis, it extruded a continuous line of molten filament onto the print bed or previous layers, following the desired path. Consequently, 1 G and high-gravity (15 G) material extrusions were obtained using the single-axis robots in the HG-MEX system.

4.2. Different gravity material extrusion

The developed system can effectively handle the extrusions of different gravity materials. To alter gravity levels in the HG-MEX

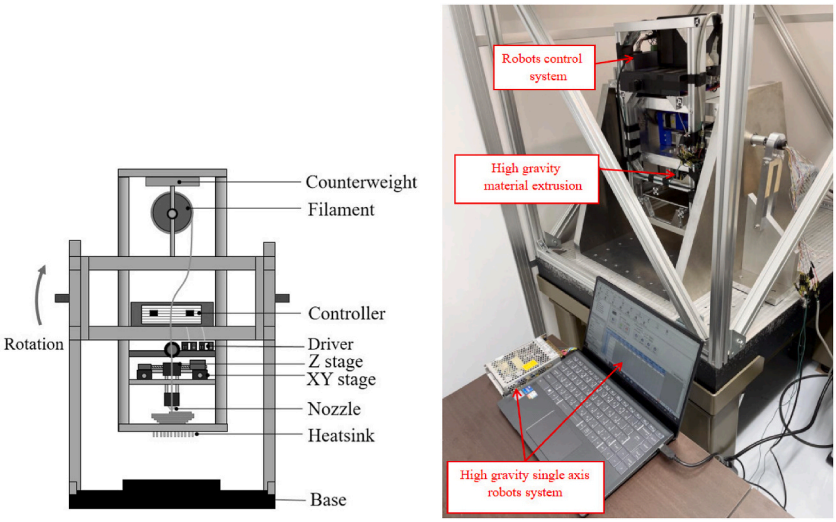

Fig. 4. Schematic of the HG-MEX machine.

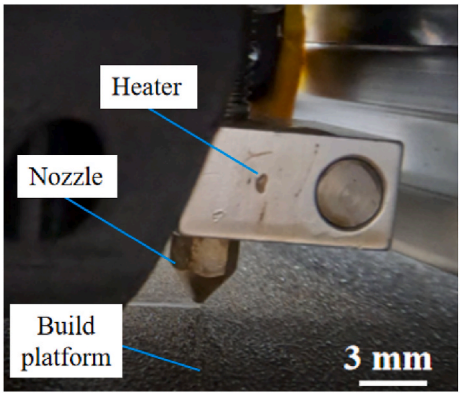

Fig. 5. Material extrusion in HG-MEX system.

system, adjustments can be implemented through the control part (VF-nC3M from Nissei Corporation), motor (G3L32N5N-PD15NVTB2 from Nissei Corporation), and driver (FMDD50D40NOM). Through parameter modifications, the driver can regulate the rotational speed of the motor. Modifications to the motor's speed facilitate changes in gravity. The control part can make control through system. The driver interprets control signals from the control part to govern the associated components. The system can extrude normally with different gravities of material extrusion, such as 1 G, 5 G, 10 G, and 15 G, demonstrating that the designed system can be reasonably used in the regular state. We focused on the state of the fabricated parts on the bottom plate, taking the size direction between the bottom board and nozzle as the research content. The movement speed of single-axis robots under high gravity can be controlled. Equation (5) delineates the correlation between resultant acceleration and rotation speed within HG-MEX systems. This equation provides insight into how alterations in rotation speed impact the gravitational forces affecting the extruded material. By manipulating the rotation speed of the HG-MEX system, we can adjust the centrifugal forces acting on the extruded material. The motor's rotational speed and torque output contribute to the modification of these centrifugal forces affecting the extruded material. Maintaining a constant rotation speed enables the attainment of various gravitational conditions for material extrusion. Fig. 6 presented an HG-MEX with a single-axis PLA robot movement speed of 16 mm/s.

Based on the results, the HG-MEX system demonstrated its capability to produce different gravity conditions through single-line

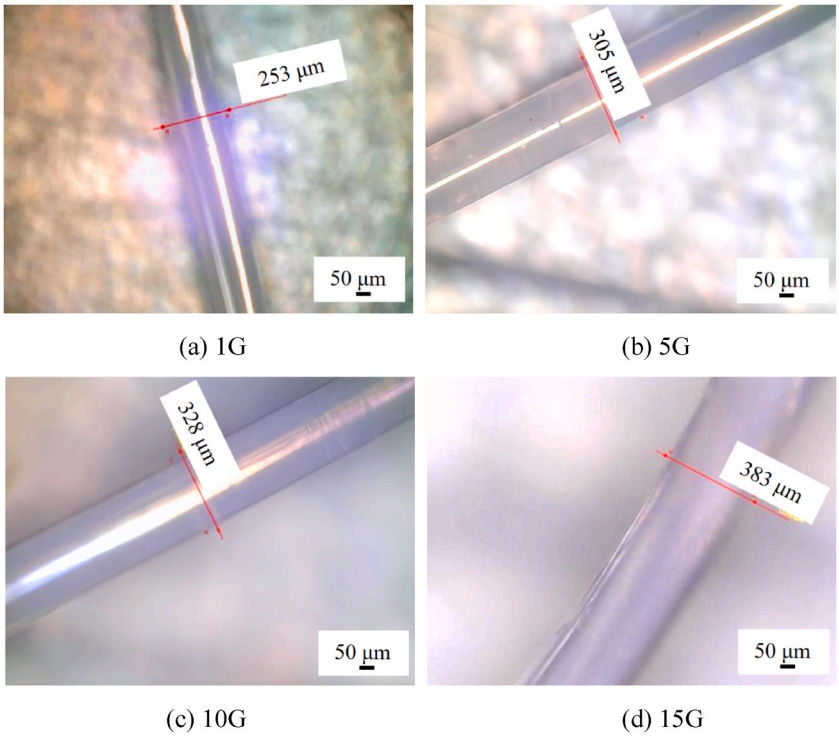

Fig. 6. HG-MEX with PLA single-axis robot with movement speed of 16 mm/s.

filament extrusion. The material extrusion process is influenced by high gravity. Fig. 6 shows the HG-MEX with a PLA single-axis robot moving at a speed of 16 mm/s. The 15 G material extrusion size is 383 μm from a side view, while that of the 1G is 253 μm. The 15 G material extrusion line was larger than that of the 1 G, providing better printing quality.

From Fig. 6, we can see the performance of material extrusion with single-axis robot movement speed of 16 mm/s. Fig. 6 (a) shows 1 G material extrusion, Fig. 6 (b) shows 5 G material extrusion, Fig. 6 (c) shows 10 G material extrusion, Fig. 6 (d) shows 15 G material extrusion. Specifically, the comparison highlights that high-gravity material extrusion demonstrates superior precision compared to standard gravity conditions. Within high-gravity environments, the extruded material encounters amplified gravitational forces, influencing its flow dynamics and deposition onto the build platform. This heightened gravitational influence fosters a more controlled and uniform extrusion process, thereby enhancing precision in the printed components. Consequently, the performance of high-gravity material extrusion showcases an elevated level of precision relative to standard 1 G gravity conditions. Gravity influences the filament behavior, and the high-gravity material extrusion performance is more uniform than that at 1 G. Fig. 7 shows the HG-MEX with a PLA single-axis robot movement speed of 20 mm/s.

Fig. 7 shows that the HG-MEX system produces varying sizes under different gravity conditions through single-line filament extrusion with single-axis robot moving at a speed of 20 mm/s. Fig. 7(a) shows 1 G material extrusion, Fig. 7 (b) shows 5 G material extrusion, Fig. 7 (c) shows 10 G material extrusion, Fig. 7 (d) shows 15 G material extrusion. The material extrusion process was influenced by high gravity. The 15 G PLA material extrusion line was larger than that of the 1 G, providing better printing quality. Gravity significantly influences the filament behavior, and the high-gravity material extrusion performance is more uniform than that at 1 G.

We obtained the extrusion performance of the PLA material under different gravity fields. Fig. 8 shows different gravity material extrusion performances at single movement speeds of 16 mm/s and 20 mm/s. In a single movement speed of 16 mm/s, we obtained the material extrusion line size L: 1 G line size is 253 μm, 5 G line size is 305 μm, 10 G line size is 328 μm, and 15 G line size is 383 μm. The ratio of increased size is around 51.4 % from 1 G to 15 G; this ratio from 5 G to 10 G is around 7.5 %; and when 10 G to 15 G, this ratio is around 16.8 %. In single movement speed of 20 mm/s, the 15G material extrusion height is 378 μm from the side view, while that of the 1 G is 177 μm. The 15G material extrusion line height was greater than that of the 1 G, providing better printing quality. In a single movement speed of 20 mm/s, we obtained the material extrusion line size L: 1 G line size is 177 μm, 5 G line size is 250 μm, 10 G line size is 322 μm, and 15 G line size is 378 μm. From 1 G to 15 G, the increased ratio is around 113.6 %; the ratio of increased size from 5 G to 10 G is around 28.8 %; and when 10 G to 15 G, this ratio is around 17.4 %. With increasing gravity, the speed of the 20 mm/s PLA material state changes became more evident, and the high-gravity PLA material extrusion performance improved.

In Fig. 8, a comprehensive analysis is provided regarding the material extrusion performances under various gravity conditions at two distinct single movement speeds: 16 mm/s and 20 mm/s. These findings are pivotal for comprehending the impact of gravity on the quality and attributes of the printed components within the HG-MEX system. At a single movement speed of 16 mm/s, it is evident

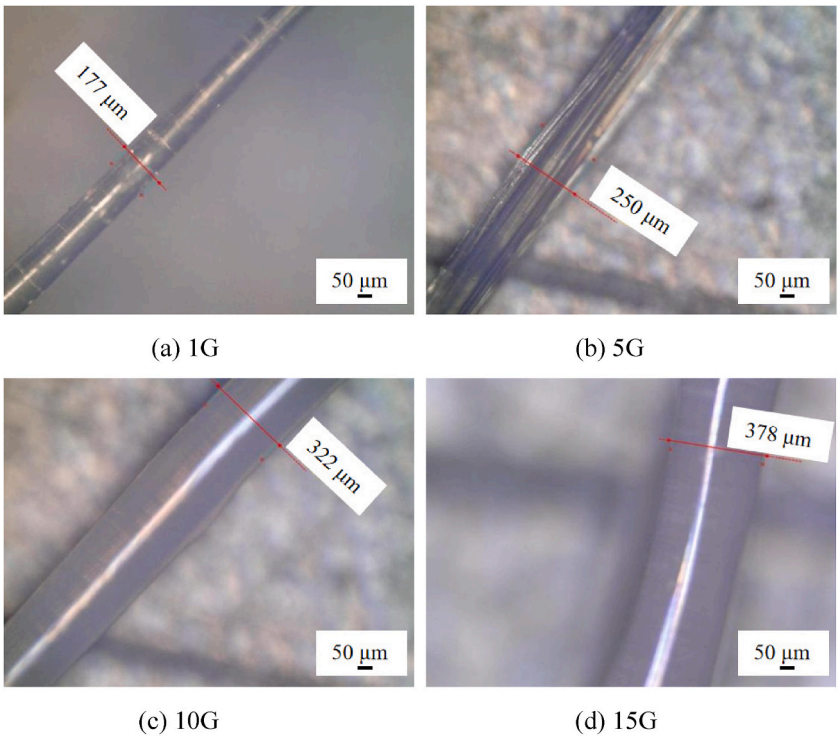

Fig. 7. HG-MEX with PLA single-axis robot with movement speed of 20 mm/s.

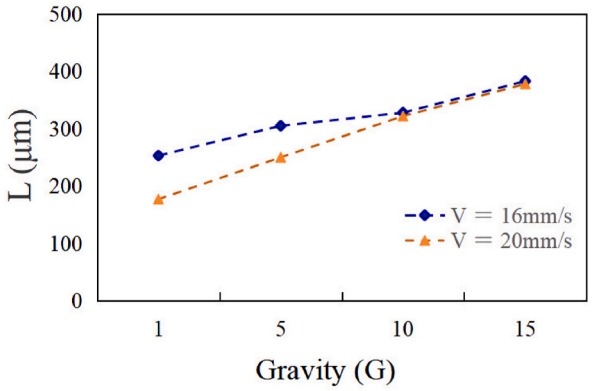

Fig. 8. Extrusion performances of different gravity PLA materials with single movement.

that the line size at 15 G significantly exceeds that at 1 G, indicating a positive correlation between gravity and extrusion size. This observed trend is further substantiated by the calculated ratios of increased size, elucidating the substantial augmentation in extrusion size with escalating gravity levels. Similarly, at a single movement speed of 20 mm/s, heightened gravity conditions result in a marked elevation in the height of the material extrusion line, particularly discernible in the comparison between 1 G and 15 G. This notable enhancement in extrusion size under increased gravity conditions underscores the potential for enhanced printing quality and performance. The findings presented underscore the pivotal role of gravity. These observed disparities underscore the significance of accounting for gravity effects in additive manufacturing processes, particularly in high-gravity material extrusion.

Based on the aforementioned findings and pertinent literature, it can be inferred that within the context of HG-MEX, both surface tension and gravity exert notable influences on the extrusion process. Gravity plays a pivotal role in influencing the stability and trajectory of the extruded filament, consequently affecting its deposition onto the build platform. Concurrently, surface tension effects contribute significantly to shaping the properties of the extruded filament, particularly in terms of its shape and diameter, as it interacts with the substrate surface. Alterations in gravity levels may consequently impact the adhesion of printed parts, with higher gravity conditions potentially enhancing material fusion and reducing defects. Drawing insights from research on the effects of variable gravity conditions, it can be deduced that gravity-induced surface tension effects play pivotal roles in governing material flow and

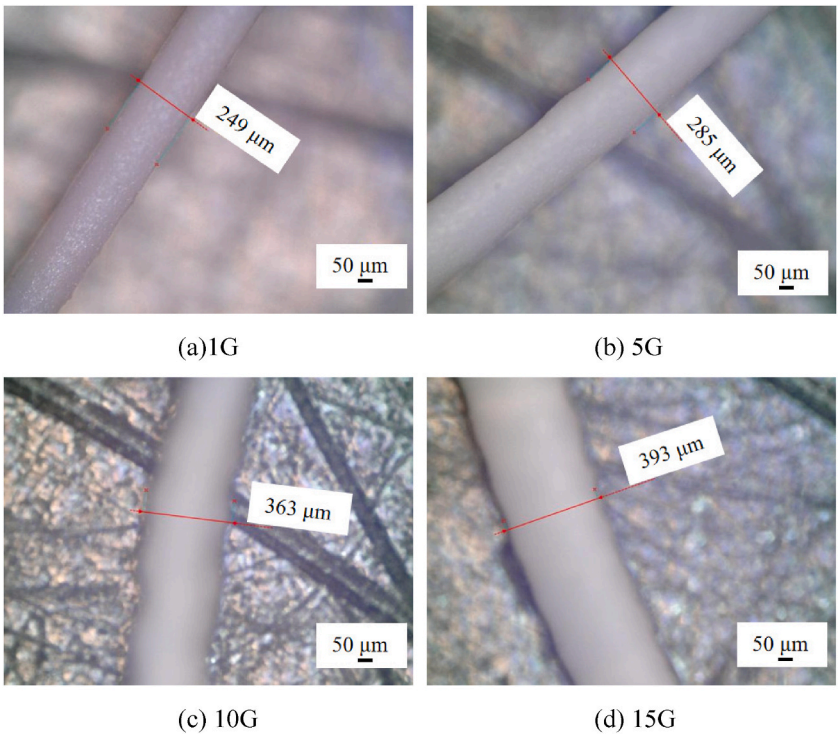

Fig. 9. HG-MEX with ABS single-axis robot (movement speed 16 mm/s).

deposition behavior within HG-MEX. Fig. 9 shows the HG-MEX with an ABS single-axis robot movement speed of 16 mm/s.

Fig. 9 shows the HG-MEX with a ABS single-axis robot moving at a speed of 16 mm/s. Fig. 9 (a) shows 1 G material extrusion, Fig. 9 (b) shows 5 G material extrusion, Fig. 9 (c) shows 10 G material extrusion, Fig. 9 (d) shows 15 G material extrusion. The 15G material extrusion size is 393 μm from a side view, while that of the 1 G is 249 μm. The 15 G material extrusion line was larger than that of the 1 G, providing better printing quality. In the current operational setting, the performance of the ABS high-gravity material extrusion demonstrates a heightened level of precision compared to conditions with standard 1 G gravity. The extrusion performance of the high-gravity ABS material was more uniform than that of the 1 G material.

Fig. 10 shows the HG-MEX with an ABS single-axis robot moving at a speed of 20 mm/s. Fig. 10 (a) shows 1 G material extrusion, Fig. 10 (b) shows 5 G material extrusion, Fig. 10 (c) shows 10 G material extrusion, Fig. 10 (d) shows 15 G material extrusion. In the HG-MEX system with ABS single-line filament extrusion, as indicated by the experimental results, the material extrusion process was influenced by high gravity. The 15 G material extrusion line was larger than that of the 1 G, providing better printing quality. Gravity significantly influences filament behavior; the high-gravity ABS material extrusion performance is also more uniform than that at 1 G.

We obtained the extrusion performance of the ABS material under different gravitational fields. Fig. 11 presents the different gravity ABS material extrusion performances with a single movement speed of 16 mm/s and 20 mm/s. In a single movement speed of 16 mm/s, we obtained the material extrusion line size of L: 1 G line size is 249 μm, 5 G line size is 285 μm, 10 G line size is 363 μm, and 15 G line size is 393 μm. At a single movement speed of 16 mm/s, the line size increased when gravity increased. From 1 G to 15 G, the increased ratio is around 57.8 %, and the ratio of increased size from 5 G to 10 G is around 27.4 %. When 10 G to 15 G, this ratio is around 8.3 %. Different gravitational material extrusion performances were obtained at a single movement speed of 20 mm/s. The 15 G material extrusion line height was greater than that of the 1 G, providing better printing quality. In a single movement speed of 20 mm/s, we obtained the material extrusion line size L: 1 G line size is 101 μm, 5 G line size is 235 μm, 10 G line size is 351 μm, and 15 G line size is 388 μm. At a single movement speed of 16 mm/s, the line size increased when gravity become higher. This ratio is around 284.2 % from 1 G to 15 G. This ratio from 5 G to 10 G is around 49.4 %, and when 10 G to 15 G, this ratio is around 10.5 %. Elevated gravity accelerates the flow velocity of the materials and concurrently augments the rate of material extrusion.

The results depicted in Fig. 11 offer ABS material manufacturing processes. At a constant movement speed of 16 mm/s, it is evident that the line size at 15 G significantly surpasses that at 1 G, indicating a notable increase in extrusion size as gravity levels escalate. This observed trend is further corroborated by the calculated ratios of increased size, emphasizing the substantial enhancement in extrusion size with heightened gravity. Moreover, the incremental impact of gravity on extrusion performance is underscored by the ratio of increased size from 5 G to 10 G. Likewise, at a constant movement speed of 20 mm/s, heightened gravity conditions result in a marked elevation in the height of the material extrusion line, particularly noticeable in the comparison between 1 G and 15 G. This noteworthy

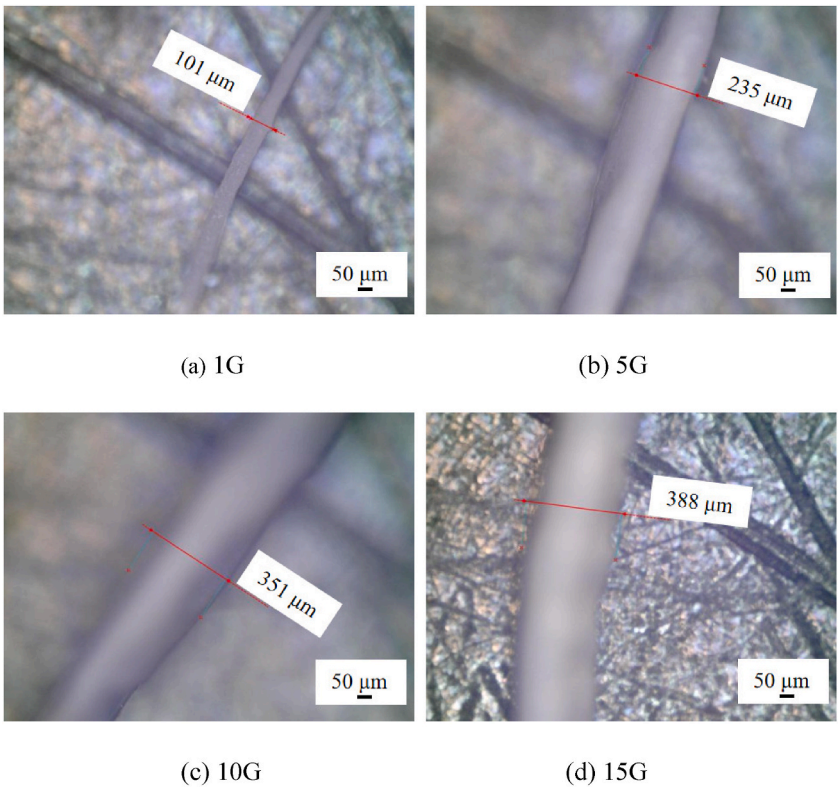

Fig. 10. HG-MEX with ABS single-axis robot movement speed of 20 mm/s.

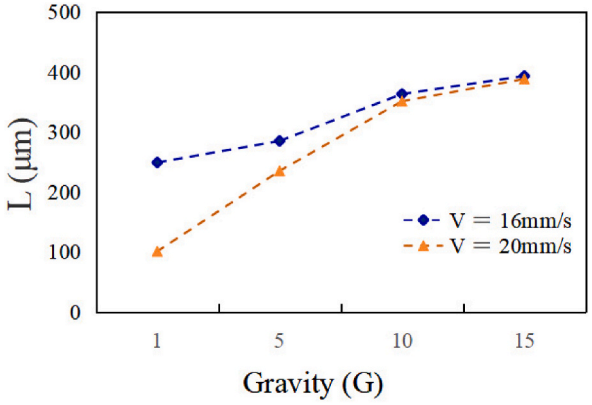

Fig. 11. Different-gravity ABS material extrusion performances with single movement.

augmentation in extrusion size under elevated gravity conditions accentuates the potential for enhanced printing quality and performance, thereby emphasizing the advantages of optimizing gravity conditions.

At elevated gravity levels, surface tension exerts discernible effects on the filament's surface characteristics, culminating in alterations in diameter, surface roughness, and stability. Gravity engenders pressure gradients within the extrusion system, thereby modulating material flow rates, velocity profiles, and pressure distribution. These gravity-induced pressure gradients significantly impact material deposition and overall print quality within HG-MEX. Moreover, surface tension effects and gravity jointly influence interfacial interactions between the extruded material and the build platform. Consequently, surface tension and gravity exert considerable influence on material properties during the extrusion process. In the context of additive manufacturing, the material is ejected from the nozzle in a molten state because of the heat applied to it, allowing it to flow and be deposited in the desired pattern and shape. As the molten material comes into contact with the build platform, it begins to lose heat to its surroundings. This cooling effect causes the material to solidify gradually, forming the desired shape layer by layer. Through Young's equation, we can find a concept for understanding the behavior of liquids on solid surfaces. When a liquid drop is placed on a solid surface, these forces determine liquid performance. In the context of material extrusion, these forces and angles become crucial for achieving accurate and consistent material deposition on a build platform. The interplay between the contact angles and surface tensions influences the behavior of the material as it solidifies and adheres to the surface, ultimately forming the desired object.

HG-MEX offers distinctive insights into the additive manufacturing process, particularly concerning how gravity influences material flow within the extrusion system. By leveraging high gravity, HG-MEX enables the examination of its impact on flow rates, thereby providing valuable insights into optimizing material deposition. Gravity's influence extends to shaping the morphology of extruded filaments and deposited layers, further enriching our understanding of material behavior. Additionally, HG-MEX facilitates the exploration of interfacial interactions between extruded layers and substrate surfaces. Comparative analysis between HG-MEX and traditional extrusion processes elucidates the unique advantages and limitations of high-gravity extrusion technology. Disparities in print quality, material properties, and process efficiency between HG-MEX and conventional methods serve as guiding parameters for further optimization and application development. Through the exploration of these physical insights, there lies a significant opportunity to advance the understanding of HG-MEX and harness gravity's potential to optimize material extrusion processes across diverse additive manufacturing applications. The experimental results for PLA and ABS confirm that high gravity promotes higher-quality printed objects. Compared with the material extrusion at 1 G, the material extrusion surface was clearer at 15 G, indicating that the HG-FDM system can produce more substantial and precise AM models.

The rationale behind high-gravity conditions lies in the intensified gravitational forces experienced by the extruded material, which, in turn, can engender heightened flow velocity and improved flow dynamics. This increase in gravitational force has the potential to compress the liquid and influence surface tension. In high-gravity environments, there is typically a shift in the Eötvös number, as gravitational forces become more predominant in comparison to surface tension forces. This alteration can have significant implications for material extrusion processes. This phenomenon fosters a more controlled and uniform material deposition process, thereby yielding smoother extrusion surfaces and diminished irregularities on the printed object. Moreover, higher gravity conditions facilitate enhanced fusion between adjacent layers of material. The augmented gravitational forces exerted on the material aid in its compression and amalgamation, thereby resulting in stronger bonding and improved structural integrity of the printed object. Furthermore, the increased gravity serves to stabilize the material flow and deposition process, consequently yielding higher-quality printed objects with reduced defects. The amalgamation of increased material flow and diminished printing defects under high-gravity conditions culminates in the production of superior-quality additive manufacturing models. The experimental results suggest that the HG-FDM device benefits significantly from the 3D printing process. By utilizing centrifugal acceleration, this approach can enhance the quality of printed objects and address the associated concerns. However, further research and development is required to validate and refine this innovation.

5. Conclusion

An innovative HG-MEX system was developed to induce a strong gravitational field during material extrusion, enabling successful material deposition. Furthermore, a system and facilities were developed to generate the desired gravity conditions for AM in high-gravity fields.

We presents the design and primary experimental results of an HG-MEX system under high gravity (15 G). PLA and ABS material extrusions were obtained in a high gravitational field. At a single movement speed of 16 mm/s and 20 mm/s, the line size become bigger with higher gravity. The high-gravity condition resulted in more material filling than the 1 G condition, leading to straighter extrusion lines. The results substantiated the improved performance achieved in such environments, confirming the characteristics and feasibility of the proposed HG-MEX system. The effectiveness of high gravity was demonstrated. The HG-MEX process enhances printing quality by fostering more uniform material flow, which in turn yields smoother surface finishes and superior layer adhesion compared to traditional material extrusion processes. Furthermore, HG-MEX facilitates faster printing speeds without compromising print quality.

The findings from HG-MEX experiments suggest that operating material extrusion processes under higher gravity conditions can yield substantial enhancements in printing quality, performance, and overall fabrication efficiency. Its innovative approach offers notable advantages over traditional material extrusion processes, thereby contributing to the advancement and widespread adoption of additive manufacturing technology. HG-MEX promotes more uniform material flow and enhances control over deposition, ultimately resulting in higher-quality prints. Moreover, in HG-MEX, a greater volume of material can be extruded simultaneously, thereby improving current printing speeds. These studies are highly significant for the development of high gravity field research, demonstrating the potential of leveraging HG-MEX processes and advancements in plastic additive manufacturing technologies. In subsequent investigations, our focus will entail enhancing system functionalities. We aim to pursue the fabrication of intricate 3D structures under conditions of high gravity. Additionally, we will explore the compatibility of HG-MEX with advanced materials, encompassing biopolymers, ceramics, and conductive polymers. Our inquiry will delve into elucidating the impact of high gravity on the extrusion process of these materials, potentially unveiling novel applications across diverse fields such as biomedicine, electronics, and aerospace.

Data availability statement

Data will be made available on request.

CRediT authorship contribution statement

Xin Jiang: Writing – review & editing, Writing – original draft, Data curation. **Ryo Koike:** Project administration, Methodology, Investigation.

Declaration of competing interest

The authors declare that they have no known competing financial interests or personal relationships that could have appeared to influence the work reported in this paper.

Acknowledgment

This study was based on the results obtained from a project at the Kanagawa Institute of Industrial Science and Technology (KISTEC).

Nomenclature

AM	Additive manufacturing
PLA	Polylactic acid
ABS	Acrylonitrile butadiene styrene
HG-MEX	High-gravitational material extrusion
E_0	Eötvös number
γ_{SL}	Solid-liquid interfacial tension ($N.m^{-1}$)
γ_{SG}	Solid-vapor interfacial tension ($N.m^{-1}$)
θ_C	Contact angle (∘)
γ	Interfacial tension ($N.m^{-1}$)
σ	Surface tensions of the involved phases ($N.m^{-1}$)
a_c	Centrifugal acceleration (m/s^2)
a_r	Resultant acceleration (m/s^2)
r_s	Distance from the center of the rotating body to build surface (m)
w_s	Rotational speed (rad/s)

References

[1] A. Nazir, O. Gokcekaya, K.M.M. Billah, et al., Multi-material additive manufacturing: a systematic review of design, properties, applications, challenges, and 3D Printing of materials and cellular metamaterials, Mater. Des. (2023) 111661, https://doi.org/10.1016/j.matdes.2023.111661.

[2] M. Popović, M. Pjević, A. Milovanović, G. Mladenović, M. Milošević, Printing parameter optimization of PLA material concerning geometrical accuracy and tensile properties relative to FDM process productivity, J. Mech. Sci. Technol. 37 (2) (2023) 697–706, https://doi.org/10.1007/s12206-023-0113-6.

[3] K.T. Estelle, B.A. Gozen, Precision flow rate control during micro-scale material extrusion by iterative learning of pressure-flow rate relationships, Addit. Manuf. (2024) 104031, https://doi.org/10.1016/j.addma.2024.104031.

[4] S. Chattopadhyay, S.D. Mohapatra, N.K. Mandal, Advancements and challenges in additive manufacturing: a comprehensive review, Engineering Research Express (2024), https://doi.org/10.1088/2631-8695/ad30b1.

[5] N. Krajangsawasdi, L.G. Blok, I. Hamerton, et al., Fused deposition modelling of fiber-reinforced polymer composites: a parametric review, Journal of Composites Science 5 (1) (2021) 29, https://doi.org/10.3390/jcs5010029.

[6] S. Vyavahare, S. Teraiya, D. Panghal, et al., Fused deposition modelling: review, Rapid Prototyp. J. 26 (1) (2020) 176–201, https://doi.org/10.1108/RPJ-04-2019-0106.

[7] M.B. Kumar, P. Sathiya, Methods and materials for additive manufacturing: a critical review on advancements and challenges, Thin-Walled Struct. 159 (2021) 107228, https://doi.org/10.1016/j.tws.2020.107228.

[8] S. Santosh, G. Nithyanandh, J. Ashwath, et al., Comparison of internal friction measurements of Ni-Ti-reinforced smart composites prepared by additive manufacturing, J. Alloys Compd. 924 (2022) 166027, https://doi.org/10.1016/j.jallcom.2022.166027.

[9] S.C. Daminabo, Grammatikos S.A. Goel, H.Y. Nezhad, V.K. Thakur, Fused deposition modeling-based additive manufacturing (3D printing): techniques for polymer material systems, Mater. Today Chem. 16 (2020) 100248, https://doi.org/10.1016/j.mtchem.2020.100248.

[10] L. Sandanamsamy, W.S.W. Harun, I. Ishak, et al., A comprehensive review on fused deposition modelling of polylactic acid, Progress in Additive Manufacturing 8 (5) (2023) 775–799, https://doi.org/10.1007/s40964-022-00356-w.

[11] S. Liu, H. Wu, B. Chao, et al., FDM preparation and properties of RGO/Ni/PLA/TPU composite materials, J. Alloys Compd. (2023) 172119, https://doi.org/10.1016/j.jallcom.2023.172119.

[12] M. Castillo, R. Monroy, R. Ahmad, Scientometric analysis and systematic review of smart manufacturing technologies applied to 3D printing polymer material extrusion systems, J. Intell. Manuf. (2022) 1–31, https://doi.org/10.1007/s10845-022-02049-1.

[13] F. Clemens, F. Sarraf, A. Borzì, et al., Material extrusion additive manufacturing of advanced ceramics: towards the production of large components, J. Eur. Ceram. Soc. 43 (7) (2023) 2752–2760, https://doi.org/10.1016/j.jeurceramsoc.2022.10.019.

[14] S.K. Romberg, A.I. Abir, C.J. Hershey, et al., Structural stability of thin overhanging walls during the material extrusion additive manufacturing of thermoset-based ink, Addit. Manuf. 53 (2022) 102677, https://doi.org/10.1016/j.addma.2022.102677.

[15] J.T. Owens, A. Das, M. Bortner, Accelerating heat transfer modeling in material extrusion additive manufacturing: from desktop to big area, Addit. Manuf. 55 (2022) 102853, https://doi.org/10.1016/j.addma.2022.102853.

[16] M.S. Kumar, M.U. Farooq, N.S. Ross, et al., Achieving effective interlayer bonding of PLA parts during the material extrusion process with enhanced mechanical properties, Sci. Rep. 13 (1) (2023) 6800, https://doi.org/10.1038/s41598-023-33510-7.

[17] F. Meng, M. Beretta, A. Selema, et al., Production and characterisation of filament-based material extrusion (MEX) additively manufactured copper parts, Procedia CIRP 121 (2024) 234–239, https://doi.org/10.1016/j.procir.2023.09.253.

[18] M.P. Neivock, C.S. Gomide, V.G. Nogueira, et al., Comparative analysis of specimen geometries in material extrusion 3D printing: implications for mechanical property evaluation, J. Appl. Polym. Sci. 141 (6) (2024) e54991, https://doi.org/10.1002/app.54991.

[19] S. Kabir, F. Mathur, A. Seyam, et al., Critical review of 3D printed continuous fiber-reinforced composites: history, mechanism, materials, and properties, Compos. Struct. 232 (2020) 111476, https://doi.org/10.1016/j.compstruct.2019.111476.

[20] X. Liu, Y. Li, L. Zeng, et al., A review of mechanochemistry: approaching advanced energy materials with greener forces, Adv. Mater. 34 (46) (2022) 2108327, https://doi.org/10.1002/adma.202108327.

[21] P. Rando, M. Ramaioli, Numerical simulations of sintering coupled with heat transfer and application to 3D printing, Addit. Manuf. 50 (2022) 102567, https://doi.org/10.1016/j.addma.2021.102567.

[22] A. Berto, M. Azzolin, S. Bortolin, et al., Condensation heat transfer in microgravity conditions, NPJ Microgravity 9 (1) (2023) 32, https://doi.org/10.1038/s41526-023-00276-1.

[23] M. Li, P. Yu, Z. Guo, et al., High-resolution and programmable line-morphologies of material-extrusion 3D printed self-leveling inks, Addit. Manuf. 71 (2023) 103582, https://doi.org/10.1016/j.addma.2023.103582.

[24] S.B. Balani, H. Mokhtarian, E. Coatanéa, et al., Integrated modeling of heat transfer, shear rate, and viscosity for simulation-based characterization of polymer coalescence during material extrusion, J. Manuf. Process. 90 (2023) 443–459, https://doi.org/10.1016/j.jmapro.2023.02.021.

[25] J. Gao, W. Rong, P. Gao, et al., A programmable 3D printing method for magnetically driven Microsoft robots based on surface tension, J. Micromech. Microeng. 31 (8) (2021) 085006, https://doi.org/10.1088/1361-6439/ac0c64.

[26] D.B. Perez, E. Celik, R. Karkkainen, Investigation of interlayer interface strength and print morphology effects in fused deposition modeling 3D-printed PLA, 3D Print. Addit. Manuf. 8 (1) (2021) 23–32, https://doi.org/10.1089/3dp.2020.0109.

[27] A. Cowley, J. Perrin, A. Meurisse, et al., Effects of variable gravity conditions on additive manufacture by fused filament fabrication using polylactic acid thermoplastic filament, Addit. Manuf. 28 (2019) 814–820, https://doi.org/10.1016/j.addma.2019.06.018.

[28] P.F. Jahromi, J. Karimi-Sabet, Y. Amini, et al., Pressure-driven liquid-liquid separation in Y-shaped microfluidic junctions, Chem. Eng. J. 328 (2017) 1075–1086, https://doi.org/10.1016/j.cej.2017.07.096.

[29] M. Amin, M. Singh, K.R. Ravi, Fabrication of superhydrophobic PLA surfaces by tailoring FDM 3D printing and chemical etching processes, Appl. Surf. Sci. 626 (2023) 157217, https://doi.org/10.1016/j.apsusc.2023.157217.

[30] L. Chen, X. Zhang, Modification of the surface quality and mechanical properties by laser polishing of Al/PLA part manufactured by fused deposition modeling, Appl. Surf. Sci. 492 (2019) 765–775, https://doi.org/10.1016/j.apsusc.2019.06.252.

[31] M.A. Quetzeri-Santiago, J.R. Castrejón-Pita, A.A. Castrejón-Pita, Analysis of contact angle for impacting droplets using a polynomial fitting approach, Exp. Fluid 61 (2020) 1–13, https://doi.org/10.1007/s00348-020-02971-1.

[32] A. Zocca, J. Wilbig, A. Waske, et al., Challenges in the technology development for additive manufacturing in space, Chin. J. Mech. Eng.: Additive Manufacturing Frontiers 1 (1) (2022) 100018, https://doi.org/10.1016/j.cjmeam.2022.100018.

[33] T. Ghidini, M. Grasso, J. Gumpinger, et al., Additive manufacturing in the new space economy: current achievements and future perspectives, Prog. Aero. Sci. (2023) 100959, https://doi.org/10.1016/j.paerosci.2023.100959.

[34] A.P. Golhin, R. Tonello, J.R. Frisvad, et al., Surface roughness of as-printed polymers: a comprehensive review, Int. J. Adv. Des. Manuf. Technol. 127 (3) (2023) 987–1043, https://doi.org/10.1007/s00170-023-11566-z.

[35] S. Gulec, S. Yadav, R. Das, V. Bhave, R. Tadmor, The influence of gravity on the contact angles and circumferences of sessile and pendant drops is a crucial historical aspect, Langmuir 35 (16) (2019) 5435–5441, https://doi.org/10.1021/acs.langmuir.8b03861.

[36] Y. Sugiura, R. Koike, High gravitational effect on process stabilization for metal powder bed fusion, Addit. Manuf. 46 (2021) 102153, https://doi.org/10.1016/j.addma.2021.102153.

[37] R. Koike, Y. Sugiura, Metal powder bed fusion in high gravity, CIRP Annals 70 (1) (2021) 191–194, https://doi.org/10.1016/j.cirp.2021.03.008.

[38] M. Kringer, A. Titz, P. Maier, et al., Effect of microgravity and reduced atmospheric pressure on manufactured photopolymer specimens, Acta Astronaut. (2024), https://doi.org/10.1016/j.actaastro.2024.01.033.

[39] X. Jiang, R. Koike, Numerical study of the effect of high gravity in material extrusion system and polymer characteristics during filament fabrication, Polymers 15 (14) (2023) 3037.

[40] J.M. Huss, A.G. Erdman, Gravity augmented fused filament fabrication additive manufacturing, J. Med. Dev. Trans. ASME 17 (2) (2023) 021003, https://doi.org/10.1115/1.4056909.
[41] A. Van Ombergen, F. Chalupa-Gantner, P. Chansoria, et al., 3D bioprinting in microgravity: opportunities, challenges, and possible applications in space, Adv. Healthcare Mater. 12 (23) (2023) 2300443, https://doi.org/10.1002/adhm.202300443.
[42] M. Petousis, N. Vidakis, N. Mountakis, Substantial mechanical reinforcement of polylactic acid with titanium nitride ceramic nanofillers in material extrusion 3D printing, Ceram. Int. 49 (10) (2023) 16397–16411, https://doi.org/10.1016/j.ceramint.2023.02.001.
[43] M. Samykano, Mechanical properties and prediction model for FDM-3D printed polylactic acid (PLA), Arabian J. Sci. Eng. 46 (2021) 7875–7892, https://doi.org/10.1007/s13369-021-05617-4.
[44] A. Das, E.L. Gilmer, S. Biria, et al., Importance of polymer rheology in material extrusion additive manufacturing: correlating process physics to print properties, ACS Appl. Polym. Mater. 3 (3) (2021) 1218–1249, https://doi.org/10.1021/acsapm.0c01228.
[45] Y. Rao, N. Wei, S. Yao, et al., A process-structure-performance modeling of thermoplastic polymers via material extrusion additive manufacturing, Addit. Manuf. 39 (2021) 101857, https://doi.org/10.1016/j.addma.2021.101857.